

## Seasonal metal fluxes derived by the interaction of surface water and groundwater in an aquaculture estuary

Xiaoxiong Wang<sup>1</sup>, Jordi Garcia-Orellana<sup>2,3</sup>, Xiaogang Chen<sup>4</sup>, Jianan Liu<sup>1</sup>, Fenfen Zhang<sup>1\*</sup>, Jianguo Qu<sup>1</sup>, Zhuoyi Zhu<sup>5</sup>, Jinzhou Du<sup>1</sup>

<sup>1</sup> State Key Laboratory of Estuarine and Coastal Research, East China Normal University, Shanghai 200062, China

<sup>2</sup> ICTA-UAB, Institut de Ciència i Tecnologia Ambientals, Universitat Autònoma de Barcelona, Barcelona E-08193, Spain

<sup>3</sup> Departament de Física, Universitat Autònoma de Barcelona, Barcelona E-08193, Spain

<sup>4</sup> Key Laboratory of Coastal Environment and Resources of Zhejiang Province, School of Engineering, Westlake University, Hangzhou 310024, China

<sup>5</sup> School of Oceanography, Shanghai Jiao Tong University, Shanghai 200030, China

Received 16 February 2023; accepted 16 June 2023

© Chinese Society for Oceanography and Springer-Verlag GmbH Germany, part of Springer Nature 2023

### Abstract

Submarine groundwater discharge (SGD) plays a major role as a conveyor of metals to coastal waters. However, the seasonal change of metal fluxes derived through SGD is unclear. Here, we evaluated the behaviours and fluxes of trace metals (Mn, Fe, Ba, Pb, U, Cr, Zn, Cu) in an estuary under different seasonal conditions. The behaviours of trace metals revealed that SGD was the source of Mn (3.51 mmol/(m<sup>2</sup>·d)), Fe (0.174 mmol/(m<sup>2</sup>·d)) and Ba (0.024 mmol/(m<sup>2</sup>·d)), but the Cu sink (−0.55 μmol/(m<sup>2</sup>·d)) and other metals exhibited a seasonal source-sink conversion. The seasonal variation of dissolved organic matter and the fresh groundwater proportion in subterranean estuaries may have an important effect on metals fluxes especially for the Fe, Mn and Ba. Our result shows that the single seasonal metal fluxes estimation applied to the annual scale will cause a large deviation, up to 3.6 times for Fe, 5.5 times for Mn, and 15 times for Ba. Therefore, the influence of seasonal fluctuations on SGD-derived metal fluxes cannot be ignored, and our findings will be important for comprehending the metal budget and cycle in nearshore environment.

**Key words:** subterranean estuary, seawater intrusion, heavy metals, seasonal changes, coastal management

**Citation:** Wang Xiaoxiong, Garcia-Orellana Jordi, Chen Xiaogang, Liu Jianan, Zhang Fenfen, Qu Jianguo, Zhu Zhuoyi, Du Jinzhou. 2023. Seasonal metal fluxes derived by the interaction of surface water and groundwater in an aquaculture estuary. *Acta Oceanologica Sinica*, 42(8): 113–124, doi: 10.1007/s13131-023-2232-4

### 1 Introduction

Submarine groundwater discharge (SGD) research has become a hotspot and attracted the attention of scientists in different fields worldwide in the past 30 years. SGD contains fresh groundwater and circulated seawater. Fresh SGD is a net material discharge process, while circulated seawater is relatively complex. The circulated seawater carries solutes that exist in the seawater to the subterranean estuaries (STE) (recharge). Depending on the residence time, solutes can be transformed or retained in the STE until they are discharged into the sea at low tide. A net increase or decrease in the chemical components existing in coastal waters is thus made possible by the STE acting as an enricher, transformer, or sink of solutes. In short, these two different components of water may play an important role in solute transport, which should not be ignored (Luijendijk et al., 2020; Santos et al., 2021). The concentrations of specific chemical components, such as trace metals, in SGD may be extremely high regardless of to the fast water flow (Mayfield et al., 2021; Wang et al., 2019; Zhang et al., 2022). This makes SGD a very important pathway for metals to enter coastal areas from land (Alorda-Kleinglass et al., 2019; Trezzi et al., 2016). These released substances

may play a very important role in the biogeochemical cycle of the ocean (Santos et al., 2011a, 2021).

SGD derived metal fluxes may be very large and may influence the trace metal reservoirs and ultimately may have a significant impact on coastal biogeochemical cycles (Beck et al., 2009; Hong et al., 2018; Kim and Kim, 2011; Shi et al., 2019; Trezzi et al., 2016). However, research on trace metal fluxes via SGD has been somewhat weak compared to studies on nutrients or carbon. Additionally, the majority of earlier studies concentrated on a single season, despite the fact that seasonal fluctuations may have a significant impact on the biogeochemical characteristics of trace metals (Berelson et al., 2003; O'Connor et al., 2018).

Seasonal changes in metal concentrations due to redox gradients, salinity and other factors in the STE can be very large, and the processes involved are complex (O'Connor et al., 2022). Fe has complex interactions with dissolved organic matter (DOM) (O'Connor et al., 2015; Waska et al., 2019), and the combination with DOM will increase the Fe mobility (de Souza Machado et al., 2016; Kim and Kim, 2015; Waska et al., 2019). These changes can occur in the intertidal zone, in which the ebb and flood of the tide cause intertidal groundwater to periodically induce changes in

Foundation item: The National Key Research and Development Program of China under contract No. 2018YFD0900702; the National Natural Science Foundation of China under contract Nos 41976040, 41976041 and 42006152.

\*Corresponding author, E-mail: ffzhang@sklec.ecnu.edu.cn

salinity, oxygen concentration, and DOM concentration (Degenhardt et al., 2021). In addition, aquaculture activity also has obvious seasonal fluctuation, and this can cause obvious seasonal changes in local biological communities and organic matter. These seasonal fluctuation would finally lead to significant changes in the biogeochemical cycling (Li et al., 2020). The large amount of organic matter derived from the significant increase in biological metabolism produces lots of manure and residues (Mendiguchía et al., 2006), which are relatively fresh and enriched in proteins, urea, etc. (Nimptsch et al., 2015). These compounds contain reducing groups (carboxyl, hydroxyl, amino, etc.) that can act as electron donors, promoting metal oxide reduction in subsurface sediments (Moosdorf et al., 2021) and resulting in migration of metals (Du Laing et al., 2009; Li et al., 2020). The subsurface estuary area is experiencing significant changes in the DOM as well as other chemical (e.g., salinity) and biological (e.g., microorganisms) variables, and these changes may also have an effect on metal fluxes (Ruiz-González et al., 2021).

Here, we hypothesized that the seasonal variation of SGD-derived metals fluxes may be significant and will strongly affect the estimation of annual metals fluxes, and finally we preliminarily discussed drivers of these seasonal changes (dissolved organic carbon (DOC) concentration and fresh-salt water ratio). We performed detailed seasonal time series observations (summer: July 2019, autumn: October 2019, spring: April 2021) of  $^{222}\text{Rn}$  and metals (Mn, Fe, Ba, Pb, U, Cr, Zn, Cu) in a typical aquaculture estuary. This study had the following aims: (1) to estimate the SGD-derived metal fluxes based on a  $^{222}\text{Rn}$  mass balance model, and the metals were classified into three categories according to their seasonal source-sink behaviour; (2) to reveal the seasonal variation and potential mechanism influencing metal dynamics in STE; and (3) to examine whether the SGD may alter the natural flux and reservoir of metals due to the influence of season, discussing the possible implications for the coastal ecological environment.

## 2 Materials and methods

### 2.1 Study site

The study site ( $5.4 \times 10^7 \text{ m}^2$ ) was in the Aojiang River Estuary ( $26.18^\circ\text{--}26.31^\circ\text{N}$ ,  $119.54^\circ\text{--}119.80^\circ\text{E}$ ), Fujian Province, which is located in southeastern China. The East China Sea is located in the eastern portion of the estuary, which has a strong tidal (the average tidal range is 3.8 m) (Peng et al., 2021). This region has a subtropical maritime monsoon climate with annual average tem-

perature of  $17\text{--}19^\circ\text{C}$ . Aojiang River is the main river in the study area and it is the sixth largest river in Fujian Province, with an average flow of  $87.7 \text{ m}^3/\text{s}$ .

In Lianjiang, aquaculture is a significant economic sector. Apart from sowing, manual thinning and harvesting, there are no other aquaculture interventions in the area and no artificial feeding. The breeds there include shellfish (*Sinonovacula constricta*, the most important aquaculture organisms), fish, shrimp, seaweed and nori (Peng et al., 2021). April is often the time for shellfish seedlings, July is the time for short-necked clam and *S. constricta* growth, and October is the time for harvest.

### 2.2 Sampling

Our field observations were performed in July 2019, October 2019 and April 2021. The groundwater samples were divided into intertidal groundwater sampling and well water sampling. The surface water samples included river water sampling, sea water sampling and time series sampling. Figure 1 illustrates the selection of sampling places. The intertidal groundwater site was gathered as close to the time series station as practicable, and the well water site was chosen as close to the shoreline as practical. To make sure that the water was properly gathered to the bottom, the well water and river water were collected with a 5 L organic glass water collector. The water samples for  $^{222}\text{Rn}$  were collected into a 2.5 L brown glass bottle through a rubber pipe (DurrIDGE, Inc., USA). The rubber pipe was inserted into the bottom of the brown bottle to ensure that there were no bubbles in the bottle (Wang et al., 2021). Shallow bores (0.5–0.6 m depth) were dug by using a spade. The bore experienced a very high groundwater discharge rate, and the water exchange immediately stabilized. After purging the bores at least three times, 2.5 L of water was collected for the analysis of  $^{222}\text{Rn}$ , and another 500 mL of sample water was stored in acid-treated HDPE bottles for subsequent sample processing.

All collected samples were processed within 24 h. The trace metals, DOC were collected at all sites, and all samples for DOC and trace metals were filtered through a membrane with an average pore size of  $0.45 \mu\text{m}$ . The DOC samples were stored in frozen conditions. Double-distilled HCl was used to acidify the trace metals below pH 2.

### 2.3 Analytical methods

$^{222}\text{Rn}$  samples were measured within one day by RAD7. The physical parameters of water were measured using a multiparameter water quality analyser (Multi 3 630 IDS, WTW, Inc., Ger-

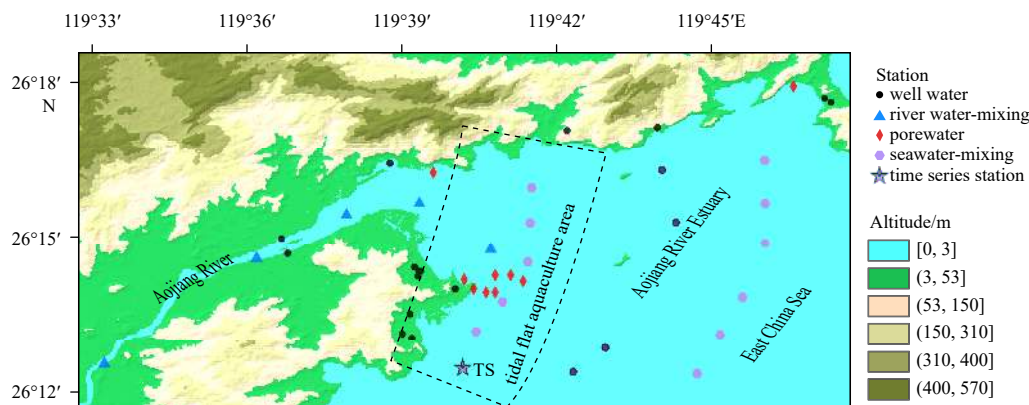


Fig. 1. Study site of Aojiang River Estuary, Fujian, China, and sampling locations distributed in this study. Five different samples are shown.

man), and these parameters included temperature, pH, salinity, and dissolved oxygen (DO). DOC was measured by the Total Organic Carbon Analyser (TOC-VCPH, Shimadzu Co. Ltd., Japan) with an error of 0.1  $\mu\text{mol/L}$  (Chen et al., 2018). The dissolved metals (dMn, dFe, dPb, dBa, dCu, dZn, dU, dCr) were measured by a high resolution inductively coupled plasma mass spectrometer (Element 2) with the addition of indium (In) as an internal standard (O'Connor et al., 2018). The relative standard deviation of all sample concentrations was less than 5% except for dCr (6.7%) and dCu (5.64%). The blank concentrations for Fe, Mn, Ba, Cu, Zn, Cr, Pb and U were 4.28  $\mu\text{mol/L}$ , 0.328  $\mu\text{mol/L}$ , 0.073  $\mu\text{mol/L}$ , 0.137  $\mu\text{mol/L}$ , 1.73  $\mu\text{mol/L}$ , 0.077  $\mu\text{mol/L}$ , 0.063  $\mu\text{mol/L}$  and 0.0004  $\mu\text{mol/L}$  respectively, and all data used in this manuscript have been deducted from the blanks. The samples were treated by direct dilution. The dilution (3% double distilled nitric acid) ratio was based on the salinity and DOC concentration to ensure that the salinity and DOC concentration of each sample were less than 1.5  $\mu\text{mol/L}$  and 60  $\mu\text{mol/L}$ , respectively.

#### 2.4 SGD flux estimation

To calculate groundwater flows, the  $^{222}\text{Rn}$ -Box model was coupled with TS station data. The  $^{222}\text{Rn}$  box model is a mass balance model, and the sources and sinks were established as equations to solve the unknown term. The sources included  $^{226}\text{Ra}$  decay ( $F_{\text{Ra-226}}$ ), river input ( $F_{\text{riv}}$ ), sediment diffusion ( $F_{\text{sed}}$ ), SGD input ( $F_{\text{SGD}}$ ), high tide input ( $F_{\text{in}}$ ); the sink items include:  $^{222}\text{Rn}$  decay ( $F_{\text{Rn-222}}$ ), atmospheric evasion ( $F_{\text{atm}}$ ), mixing loss ( $F_{\text{mix}}$ ), ebb tide output ( $F_{\text{out}}$ ) (Burnett and Dulaiova, 2003; Zhang et al., 2016). In which high and low tides are combined for  $^{222}\text{Rn}$  inventory to become the tidal contribution.

The specific calculation methods can be found in supporting information (Supplementary  $^{222}\text{Rn}$  Box model), and related parameters are presented in Table S1.

### 3 Results

#### 3.1 Seasonal variation of salinity and $^{222}\text{Rn}$

The salinity of intertidal groundwater ranged from 24.9–25.7 (mean 25.2), 12.5–14.3 (mean 13.5), 28.5–29.3 (mean 28.9) in July, October and April, respectively. The salinity in seawater in July, October and April was 3.95–26.2 (mean 18.5), 25.9–29.6 (mean 27.2), and 21.8–31.3 (mean 27.2), respectively. Other parameters, such as DO, pH, and oxidation-reduction potential (ORP) were listed in Table S2.

The average  $^{222}\text{Rn}$  activity of each endmember showed a clear trend of well water > intertidal groundwater > river water > seawater (Fig. 2). Although a seasonal variability was also noted, spatial variability stood out more. The range of  $^{222}\text{Rn}$  activity in the intertidal groundwater in July, October and April was 5 200–7 400  $\text{Bq/m}^3$  (mean 6 400  $\text{Bq/m}^3$ ), 1 500–13 000  $\text{Bq/m}^3$  (mean 6 100  $\text{Bq/m}^3$ ), and 1 800–5 800  $\text{Bq/m}^3$  (mean 3 300  $\text{Bq/m}^3$ ), respectively.

#### 3.2 Seasonal variation of dissolved metals and DOC

The metals concentrations also varied greatly in space and time. Higher concentrations of dMn, dFe, dBa and dPb were observed in intertidal groundwater than in seawater, while dCu and dU showed the opposite relationship regardless of seasons (Fig. 3).

The concentration of DOC also exhibited strong seasonal and spatial variations. The DOC concentration in intertidal groundwater was 234  $\mu\text{mol/L}$ , 208  $\mu\text{mol/L}$  and 125  $\mu\text{mol/L}$  in July, October and April, respectively. The average concentration of DOC in seawater was 173  $\mu\text{mol/L}$ , 117  $\mu\text{mol/L}$  and 93  $\mu\text{mol/L}$ , respect-

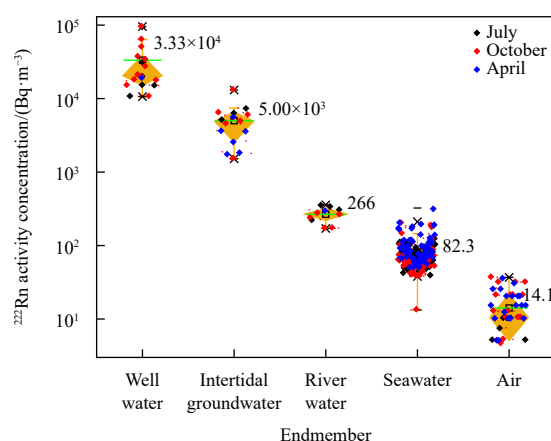


Fig. 2. The average  $^{222}\text{Rn}$  activity concentration of each endmember in three season. The box plot shows the  $^{222}\text{Rn}$  activity concentration range of the corresponding endmember and the green line is the average value.

ively. In the corresponding season, the concentration of DOC in intertidal groundwater was consistently higher than that in seawater.

#### 3.3 Time series observation

Approximately 27 h of time series observations provided information on various physical and chemical parameters and  $^{222}\text{Rn}$  activity (Fig. 4). In July, October and April, the  $^{222}\text{Rn}$  activities were 40–126  $\text{Bq/m}^3$  (mean 73  $\text{Bq/m}^3$ ), 38–201  $\text{Bq/m}^3$  (mean 70  $\text{Bq/m}^3$ ), and 58–131  $\text{Bq/m}^3$  (mean 92  $\text{Bq/m}^3$ ), respectively. The water depth ranged from 0 to 5.28 m (mean 2.63 m), 0.55–4.90 m (mean 2.90 m) and 0.27–6.96 m (mean 3.84 m), and the wind speed was 0–6.4 m/s (mean 2.2 m/s), 3.2–11.2 m/s (mean 6.1 m/s), and 0.0–6.40 m/s (mean 2.2 m/s), respectively. Nearly all characteristics varied with the tide, however the range of variation varied from season to season (Fig. 4). According to principal component analysis (PCA, IBM, SPSS Statistics, Version 23) and correlation analysis, the metal and physicochemical factors were split into two groups that, respectively, were linked to independent from tidal changes. The components closely related to tidal changes include  $^{222}\text{Rn}$  (-), Mn (-), Zn (+), Cu (-), and Fe (-) in July;  $^{222}\text{Rn}$  (-), Cr (-), Fe (-), Cu (-), and Ba (-) in October; and Pb (+), U (+), Fe (-), Cu (-), Mn (-), and Ba (-) in April (-: opposite to tidal change, +: same as tidal change) (Fig. 4).

#### 3.4 Metal addition and removal

Each metal has significant addition and removal (Fig. 5). Mn, Fe, Ba, and Pb all showed obvious additions in the medium salinity (7–28), but Pb was less visible than the other three metals. While Zn, U, and Cr had major seasonal shifts in removal and addition, Cu was strongly eliminated during each of the three seasons. The variation for each metal concentration with salinity was also different, and there were seasonal variations. The concentrations of Mn and Ba were negatively correlated with salinity in all seasons, while the concentration of U was positively correlated with salinity in all seasons. All other metals exhibited seasonal variability.

### 4 Discussion

#### 4.1 Seasonal SGD flux and its composition

When analysing metal fluxes through SGD, calculating SGD

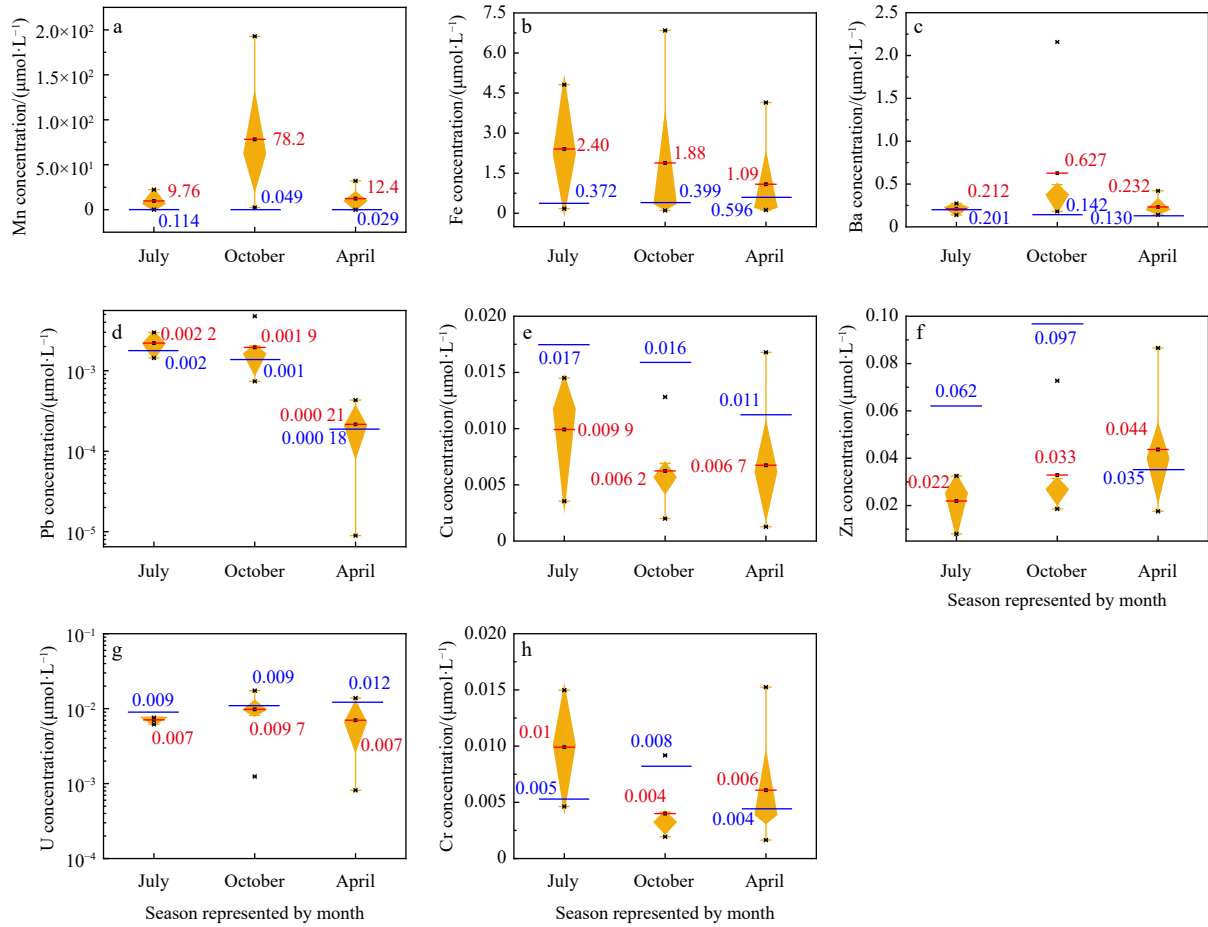


**Fig. 3.** Average concentrations of dissolved metals (dMn (a), dFe (b), dBa (c), dPb (d), dCu (e), dZn (f), dU (g) and dCr (h)) in intertidal groundwater (box plot in yellow, red line is the mean value) and seawater (blue line).

flux is a crucial step. It also might be an important factor in managing metal fluxes. The <sup>222</sup>Rn box model was used to estimate SGD flux, mainly based on the <sup>222</sup>Rn activity show a clear trend in different endmember (Fig. 2). Assuming that radon will equilibrate with the nearshore groundwater throughout the transfer from the continental groundwater (Chen et al., 2018), we choose intertidal groundwater (average value) as the most representative groundwater endmember. In addition, an approximate inverse correlation between tidal variation and <sup>222</sup>Rn activity in time series observation (Figs 4a–c) was observed, which indicates that tidal pumping may be an important factor driving SGD flux.

The source and sink terms of the <sup>222</sup>Rn Box model are shown in Table 1. The average flux of SGD in July, October and April was 14.0 cm/d, 9.45 cm/d and 14.9 cm/d, respectively. The SGD fluxes show very large short-term variability but little seasonal variability (Table 1 and Fig. S2). Because of this, we only calculated the daily flux, not the hourly flux, in the following calculations to prevent the introduction of excessive standard deviation; that is, we assumed that the daily SGD flux did not change much in the same season.

The intertidal groundwater here represents the total SGD, which is influenced by two components, one for recirculated seawater and the other for fresh groundwater (Nakajima et al., 2018). So we distinguish between the ratio of salt water and fresh water in intertidal groundwater, not in seawater. To calculate the brackish and fresh SGD ratios, we used the simplest salinity model (two-terminal endmember) between intertidal groundwater

and seawater to estimate (Hagedorn and Tsuda, 2022; Santos et al., 2009, 2011b):

$$1 = f_s + f_f, \quad (1)$$

$$S_p = S_s f_s + S_f f_f, \quad (2)$$

where  $f_s$  is the proportion of recirculated seawater,  $f_f$  is the proportion of fresh groundwater,  $S_p$  is the average salinity of intertidal groundwater (the salinity was 25.2, 14.3 and 28.9 in July, October and April, respectively),  $S_s$  is the salinity of seawater in the mixing zone (the salinity was 27.1, 27.1 and 31.1 in July, October and April, respectively) and  $S_f$  is the salinity of fresh groundwater. The proportion of seawater is:

$$f_s = \frac{S_p}{S_s}. \quad (3)$$

However, there is a problem here that the region is an estuarine area, the river water can be involved in this mixing. If river water is added, then it will become a three-terminal endmember. And the existing parameters are not enough to support the model. In order to solve this problem, we did not choose the salinity of the outer seawater when choosing the salinity of the seawater endmember, but used the salinity of the surface water at the intertidal groundwater sampling station instead. In this way, the salinity of  $S_s$  may be low due to the mixing of river water and seawater, which leads to a high proportion of  $f_s$ . In our calculations, the

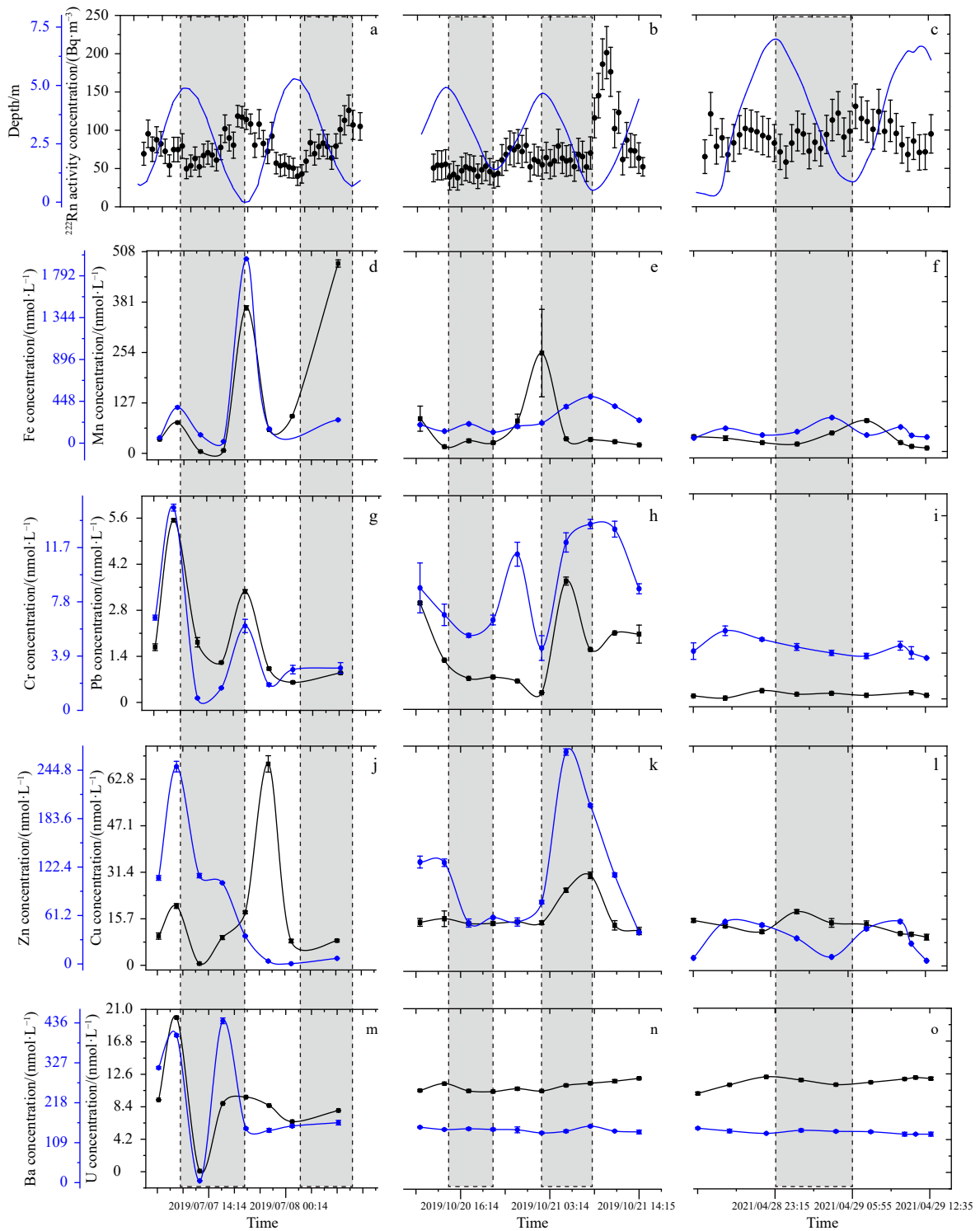


**Fig. 4.** Time series results of the water column depth,  $^{222}\text{Rn}$  activity concentration, Fe, Mn, Cr, Pb, Zn, Cu, Ba and U in July 2019, October 2019 and April 2021. Other parameters (DO, pH, temperature, and salinity, DOC, DIC and DSi) of time series observation are shown in Fig. S1. The areas circled by dash dot line represent periods of ebb tide.

proportion of brackish water in both July and April is 93%, which is very close to the recommended value (~90%) in the literatures (Burnett et al., 2003; Taniguchi et al., 2006). The percentage of salty water in October is only 53%, which is not due to the change of surface seawater salinity (surface water salinity was 27.1, 27.1, and 31 in July, October, and April, respectively), but to the lower salinity of intertidal groundwater in this season, with a maxim-

um salinity of only 14.3. Finally, the proportions of circulated seawater in July, October and April were 0.932, 0.529 and 0.931, respectively, and it also show a clear seasonal difference.

#### 4.2 Seasonal metal fluxes derived by SGD and its potential reasons

The SGD-derived metal fluxes are shown in Fig. 6 (Table S3 in

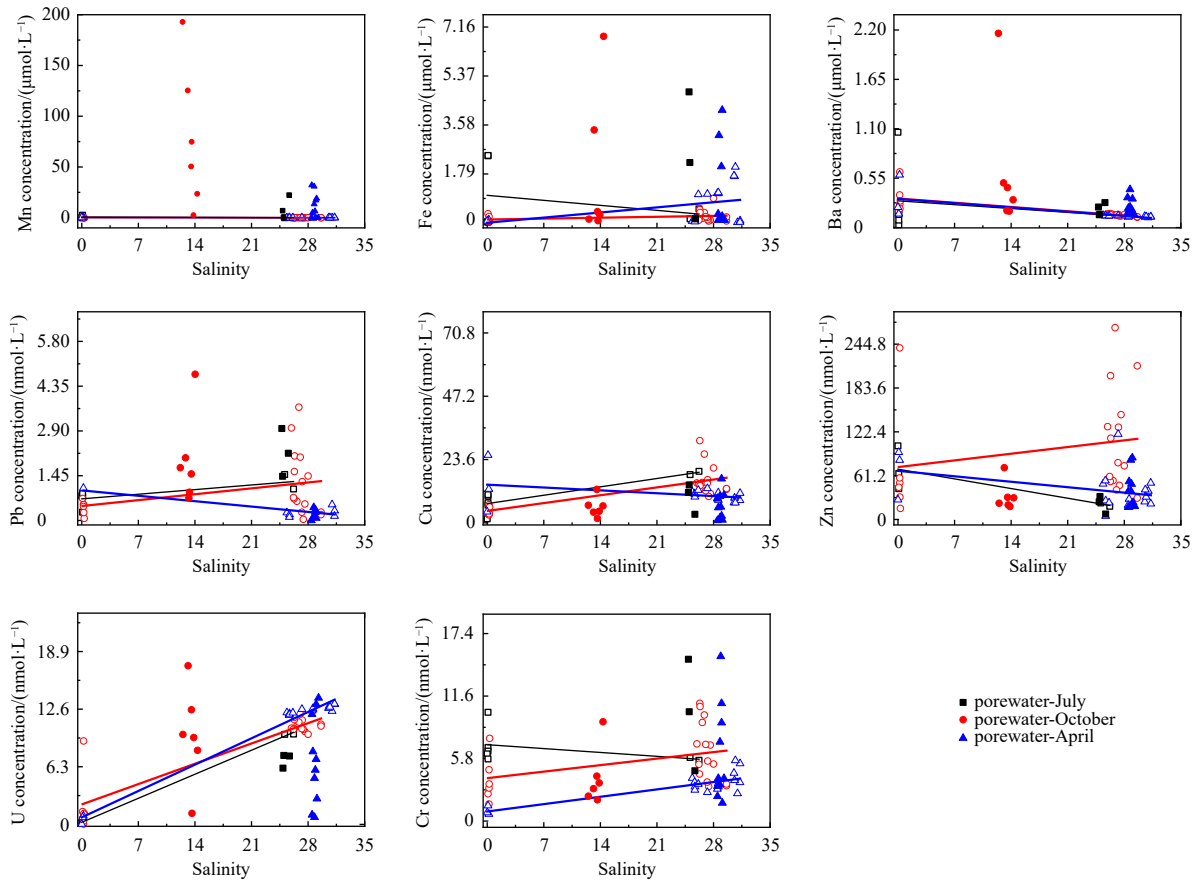


**Fig. 5.** Relationship between salinity and metal concentrations in well water, intertidal groundwater and seawater. The black symbol represents July, red symbol represents October, blue represents symbol April. The symbol of the fill colour represents the intertidal groundwater sample, the hollow symbols where the salinity close to zero represent the well water samples, and the rest is seawater sample. The line is the mixing line of two endmembers (well water and seawater).

**Table 1.** Sources and sinks of  $^{222}\text{Rn}$  fluxes ( $\text{Bq}/(\text{m}^2\cdot\text{h})$ ) in July, October and April

	July 2019	October 2019	April 2021
<b>Sinks</b>			
Atmospheric evasion	$1.49 \pm 2.09$	$5.02 \pm 1.61$	$1.37 \pm 1.26$
Mixing loss	$26.9 \pm 2.31$	$25.6 \pm 3.65$	$45.9 \pm 1.37$
Tidal contribution	$3.20 \pm 0.301$	$-1.50 \pm 0.467$	$1.90 \pm 1.15$
$^{222}\text{Rn}$ decay	$0.01 \pm 0.006$	$0.02 \pm 0.009$	$0.04 \pm 0.022$
Total	31.6	30.6	49.2
<b>Sources</b>			
River input	$2.20 \pm 0.493$	$0.491 \pm 0.10$	$1.66 \pm 0.489$
SGD input	$35.1 \pm 3.28$	$29.5 \pm 2.57$	$43.8 \pm 2.06$
Sediment diffusion	$1.27 \pm 0.553$	$1.94 \pm 0.772$	$0.70 \pm 0.161$
$^{226}\text{Ra}$ decay	$0.0974 \pm 0.0636$	$0.1060 \pm 0.0496$	$0.1540 \pm 0.0853$
Total	38.1	32.0	46.3
$V_{\text{SGD}}/(\text{cm}\cdot\text{d}^{-1})$	$14.0 \pm 4.45$	$9.45 \pm 0.974$	$14.9 \pm 3.70$

Note:  $V_{\text{SGD}}$  is SGD flux.

supporting information for specific data). Following is the calculation method (Wang et al., 2019):

$$F_{\text{metal}} = V_{\text{SGD}} \times \text{Metal}_{\text{intertidal groundwater}} - V_{\text{SGD}} \times \phi_r \times \text{Metal}_{\text{seawater}} \quad (4)$$

We assume that all parameters used here are in steady state during the season.  $F_{\text{metal}}$  is the metal net fluxes of SGD ( $\text{mmol}/(\text{m}^2\cdot\text{d})$ ),

$V_{\text{SGD}}$  is the SGD flux ( $\text{m}/\text{d}$ ),  $\phi_r$  is the proportion of circulated seawater in SGD, and  $\text{Metal}_{\text{intertidal groundwater}}$  and  $\text{Metal}_{\text{seawater}}$  are the average metal concentrations in the intertidal groundwater and seawater

SGD-derived metal fluxes display obvious seasonal variations and vary widely between different metals. This is also seen in the time series observation, and different metals' variations with the tide over various seasons have visibly different amplitudes and

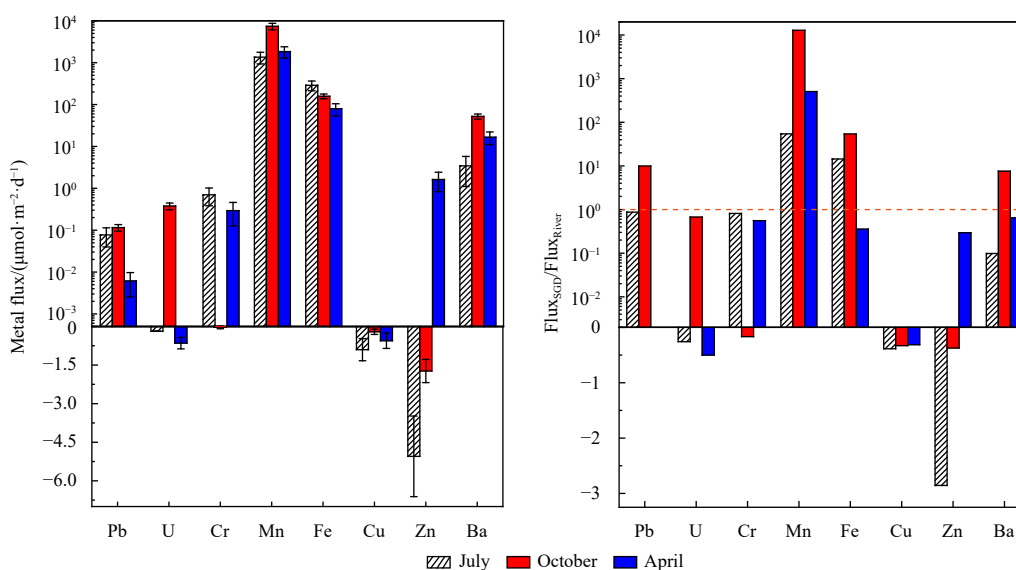


**Fig. 6.** Metal fluxes histogram through submarine groundwater discharge (SGD) in three seasons (a); the negative values indicate that metal fluxes are net input from sea to land. Ratio of metal fluxes through groundwater to through river (b). The dotted orange line indicates that the metal fluxes through the SGD is equal to the flow through the river, the negative value is caused by the negative metal fluxes derived from SGD. The Cr flux in October is relatively small ( $0.038 \mu\text{mol}/(\text{m}^2\cdot\text{d})$ ), so it cannot be seen. The Pb flux of river in April is not shown because the Pb concentration is below detection in this season.

trends (Fig. 4). The concentrations of metals in July and October (except U and Ba) are inversely correlated with the tide level (Figs 4d, e, g, h, j, k, and m), while in April is totally different (Figs 4f, i, l, and o).

While some metals, such as Fe, Mn and Ba are supplied to the sea through the SGD, others, such as Cu, are removed from the water column or behave seasonally (Zn, U, Cr). According to their source-sink behaviour, the eight metals are divided into three categories: supply metals (Fe, Mn, Ba), remove metals (Cu) and dynamically balance metals (Zn, U, Cr, Pb).

As Eq. (4) shows, the SGD flux may also be the reasons for driving metal fluxes change. However, the variation in SGD flux is not obvious (Table 1), and the seasonal trend of SGD flux (April > July > October) has no consistent relationship with the flux of any metals (Fig. 6). Thus, the main factor controlling the seasonal variation of SGD-derived metal fluxes should be due to the concentration difference of metals between seawater and intertidal groundwater and should not be due to the SGD flux variation.

The supply metals (Fe, Mn and Ba) by SGD are generally with additions or their concentration is negatively correlated with salinity (Fig. 5). For example, Mn has obvious addition, and its concentration is negatively correlated with salinity (the concentration of Mn in well water is higher than that in seawater). The removal metal (Cu) by SGD is closely related to its strong removal behaviour in all three seasons (Fig. 5). Cr, Zn and U show significant seasonal differences in addition and removal, and their fluxes also show seasonal changes.

#### 4.2.1 Supply metals

SGD-derived Mn, Fe and Ba fluxes are positive in three seasons. These three metals are added in the medium salinity, which may be due to the metal oxide dissolution or desorption from the sediment. So, we paid special attention to the factors influencing the addition and removal behaviour of metals.

The presence of oxygen or sulphide, etc., can affect the redox state of the interstitial layer. Unfortunately, we only got the DO

and ORP in surface seawater and did not obtain the vertical value of DO and ORP in the intertidal groundwater layer. However, as far as we know, in STE, the vertical change of DO is drastic (so is ORP), which is the same regardless of the season (low DO in deep groundwater is due to long residence time) (O'Connor et al., 2018), and DO in deep groundwater is generally at a low level, while DO in near surface is higher. However, in this research, we focused on the seasonal change on metal behaviour in the surface layer, so the surface environment was paid special attention. In addition, the response of the surface waters for season should be greater than deep STE, so we think the DO in surface waters may be of greater concern. In this study, the oxygen content in the upper floating water was always relatively high (mean value  $\geq 6.26 \text{ mg/L}$ ), and its impact on the Mn and Fe supply cannot be ignored. However, due to the small difference in oxygen in the upper floating water in the three months ( $6.26 \text{ mg/L}$ ,  $6.93 \text{ mg/L}$ ,  $7.22 \text{ mg/L}$  in July, October and April, respectively), oxygen had little influence on the seasonal difference in Mn and Fe emissions from STE. Sulphide was not considered in this study because this region is a sandy coast with less vegetation, there was no smell of hydrogen sulphide in any water body (Charette et al., 2005), and the Fe content in intertidal groundwater was very high in three seasons (Fig. 3), which also seems to account for the lower content of  $\text{S}^{2-}$ .

Given that we only have surface water ORP data, and although the surface ORP data are sufficient to explain our main questions, the fluctuation of subsurface and deep ORP may also be relevant for our metal research, particularly for the investigation of redox-sensitive metal cycling mechanisms in interstitial aquifers. This is a limitation of the current study.

Fe is highly mobile when in the form of  $\text{Fe}^{2+}$  (Charette et al., 2005). DOM plays an important role in Fe migration (Waska et al., 2019). Since DOM is a strong reductant and has a variety of reducing functional groups, such as hydroxyl, phenolic compounds and amino compounds (Li et al., 2020; Nimptsch et al., 2015; Santana-Casiano et al., 2014), which can reduce Fe or form

organometallic complexes. Considering this, can the DOM also affect the migration of Fe seasonally?

The reason for the association with aquaculture is that DOM concentration here may be related to aquaculture (Wang et al., 2017). This study area is a typical aquaculture area (*S. constricta*, seaweed, nori and so on), and the seasonal changes in aquaculture stage (seedling, maturity, after harvest of clams) are very large, so the DOC concentration and composition may also vary greatly. In July, during clam maturity, there was a large number of benthic organism ([http://hyyyj.fujian.gov.cn/xxgk/tjxx/201912/t20191211\\_5148836.htm](http://hyyyj.fujian.gov.cn/xxgk/tjxx/201912/t20191211_5148836.htm)). The metabolism of these organism can produce fresh organic matter that was highly reducible (O'Connor et al., 2018) (urea, etc.). Not only that, but the DOC concentration may also exhibit seasonal variations. This is the reason why we chose these three seasons. The highest DOM concentration was found in July, corresponding to the maturation period of clams; a lower DOM concentration was found in October, corresponding to the post-harvest period of the economic organisms, and the lowest DOM concentration in April, corresponding to the seeding period of the clams. There are clear seasonal variations in DOM concentration and composition between periods (Hao, 2021), so that a natural concentration gradient is formed, which facilitates the examination of the characteristics of metal behavior associated with DOM.

The relationship between DOM and aquaculture was also verified by another group of culture experiments (Hao, 2021). This experiment was performed at the same time as ours and in the same area, with an incubation time of 1 h. The culture experiment of shellfish proved that its metabolism can significantly contribute to active DOM (for example, the urea concentration in the feeding group was 1.3 times that of the blank group, the DOC concentration in feeding group was 1.12 times that of the blank group, and the DON concentration in feeding group was 1.58 times that of the blank group). The researchers also pointed out that the excretion or release of benthic organisms is an important source of glycine. Smaal and Vonck (1997) reported that farmed mussels can contribute significant amounts of dissolved organophosphates. The comparison between the aquaculture area and the nonaquaculture area showed that the urea content in the aquaculture area was higher. In any case, aquaculture organisms, as the dominant group of organisms in this region, may have an impact on local productivity, and may modify or at least provide some fresh organic matter (old carbon is generally not highly reactive) and promote Fe reduction in groundwater. Al-

though we have not observed the interaction between DOC and Fe at the micro level, Fig. 7 proves that the increase of seasonal DOC concentration will lead to the increase of Fe flux driven by SGD.

The seasonal variation in the average Fe concentration in intertidal groundwater is correlated with the seasonal variation in the DOC concentration both in intertidal groundwater and in seawater (Fig. 7). This suggests that an increase in DOC is associated with an increase in SGD-driven Fe flux. Similar result was found in other study (O'Connor et al., 2018). Waska et al. (2019) found that most DOM bound with iron came from marine sources, which indicated that marine DOM could affect the Fe migration at the molecular level. DOM produced by these aquaculture organisms entered the intertidal groundwater layer through tidal pumping (Santos et al., 2009, 2011a), which in turn interacts with Fe in the sediment and promotes Fe transport.

Although both Mn and Fe migration and solubility are controlled by redox, Mn and Fe change very differently in intertidal groundwater, and their redox abilities also differ (Charette et al., 2005). The seasonal changes in Mn ( $R^2 = 0.019$ ,  $r = 0.184$ ,  $p = 0.144$ ) and Ba ( $R^2 = 0.008$ ,  $r = 0.156$ ,  $p = 0.220$ ) supply do not appear to be related to DOC concentrations. So there are large seasonal differences between Mn and Fe fluxes derived from SGD.

Because of the fluxes of Mn and Ba are not correlated with the DOC concentration, the controlling factors of Mn and Ba fluxes may be different from Fe. An interesting phenomenon is that the seasonal variation of SGD-driven Mn and Ba fluxes is very similar (Fig. 8). This is probably because Ba may be dissolved/desorbed along with the dissolution of Mn oxides (Charette and Sholkovitz, 2006). Considering that Mn is also a redox-sensitive metal, the large increase of Mn concentration could be related to the low ORP. However, as stated above, Mn exhibits different characteristics from Fe (weak relationship with DOC). And surface water is generally characterized by high ORP and high DO (except for DOM which is reductive), so the increase of Mn concentration is not related to surface water. The fresh groundwater should be expected to play a major role. Gonneea et al. (2014) pointed out that fresh groundwater can increase Mn flux, as fresh groundwater has a long residence time and low oxygen. Figure 8 also shows that the flux of Mn responds high in quarters with a high percentage of freshwater and this difference is evident.

In addition,  $^{222}\text{Rn}$  activity was significantly correlated with Mn ( $R^2 = 0.468$ ,  $r = 0.692$ ,  $p < 0.0001$ ,  $n = 49$ ) and Ba ( $R^2 = 0.455$ ,  $r =$

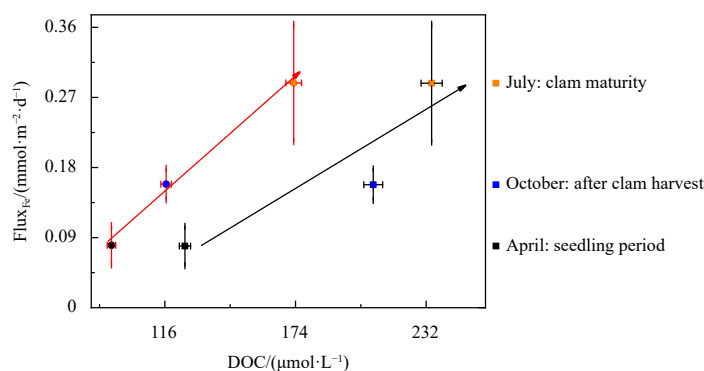


**Fig. 7.** The relationship between dissolved organic carbon (DOC) concentration of seawater (circle) and intertidal groundwater (square) and Fe flux in submarine groundwater discharge (SGD) and the corresponding aquaculture stage (the black colour represents the seedling period ( $n = 3$ ), blue represents after clam harvest ( $n = 6$ ), orange represents clam maturity ( $n = 10$ )), since each point represents of one field observation, we observed three seasons, so there are only three points. The arrow indicates that the Fe flux driven by SGD increases with the increase of DOC concentration.

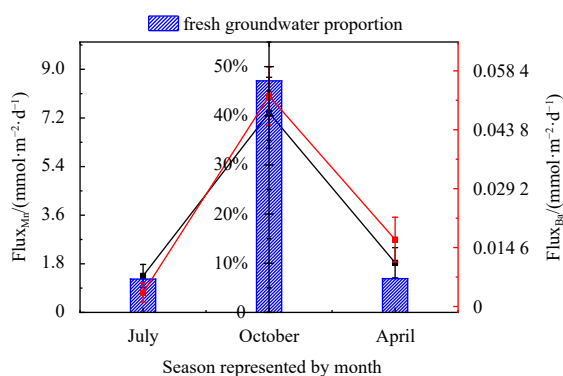


**Fig. 8.** Mn and Ba fluxes derived through SGD in different seasons, the blue shaded histogram represents the proportion of fresh water in groundwater.

0.683,  $p < 0.0001$ ,  $n = 49$ ) (Fig. 9), and  $^{222}\text{Rn}$  itself is an excellent tracer for groundwater and its activity in fresh groundwater is very high (the average activity in well water is nearly an order of magnitude higher than that of intertidal groundwater, Fig. 2) (Santos et al., 2010). These also indicate that the fresh groundwater may be an important factor controlling Mn and Ba fluxes. The low oxygen content fresh groundwater may reduce the manganese oxide, and then results in an increase in Mn concentration. Ba is often combined with Mn oxides (in our results, only Mn and Ba have the strongest correlation), and with the dissolution of Mn oxides, Ba is also released so that the flux of Ba in groundwater also increases.

#### 4.2.2 Removal metal

As shown in Fig. 6, Cu fluxes were negative (sinking in the STE) in all three seasons. The concentration of Cu in intertidal groundwater was significantly lower than that in surface seawater in all seasons. Considering that Cu is an essential element for biological growth, we assumed that the aquaculture may be responsible for the removal of Cu. Intensive *S. constricta* and shellfish cultivation and other filter-feeding organisms absorb and enrich bio-beneficial elements in their growth stage. The benthic demand (Amato et al., 2016; Shine et al., 1998) made the concentration of Cu in intertidal groundwater very low in any season and causing continuous Cu removal during harvesting.

We performed culture experiments to verify shellfish (one of the main cultured species) were collected near the intertidal groundwater site (Fig. 1) and placed in an incubator. *In situ* seawater was added to simulate the natural environment, and the

incubation time is set to 1 h (Hao, 2021). Nothing else is added during this period. The location of the capture experiment was carried out on the shore closer to the sampling point to simulate the *in situ* environmental conditions (temperature, light, etc.). When sampling, re-stir the water sample for sampling. The water samples at the beginning and after shellfish capture were collected for analysis. The result showed that benthic organisms can capture Cu (the Cu concentration in seawater was  $0.012 \mu\text{mol/L}$  at the beginning, and  $0.01 \mu\text{mol/L}$  after capture experiment. Finally, the Cu concentration decreased by 25.3%). This process makes Cu concentration in the intertidal groundwater lower than that in the seawater, thus making Cu sink in STE. Since these benthic organisms were eventually harvested, the Cu was taken out of the original environment, causing complete removal of Cu.

#### 4.2.3 Dynamically balance metals

The Pb fluxes are all positive, but their values are small. Considering the concentration of Pb in intertidal groundwater is similar to that in seawater and the error, we classify Pb as a dynamic equilibrium metal. In addition, Pb also exhibits different behaviour from that of Mn, Ba and Fe. Shahid et al. (2012) pointed out that Pb can combine with DOC to form organic-Pb, but this was not found in our observation.

The Cr, U and Zn flux derived from SGD show greatly seasonal differences, especially they all have source-sink conversion. In some seasons, groundwater releases it into seawater, while in other seasons, the opposite occurs. Many physicochemical properties and biological changes alter with the seasons, and these changes may affect the source-sink characteristics of certain metals in STE. In addition, as seen in Fig. 3, the concentrations of Zn, Cr and U in intertidal groundwater and seawater are similar, indicating that these three metals may be in a state of dynamic equilibrium. Zn is a biologically active element which can be metabolized by organisms and catalysed by enzymes (Amato et al., 2016). Therefore, Zn can be taken up and used by biology. As for why Zn and Cu behave slightly differently, our explanation is that the concentration of Cu and Zn in intertidal groundwater is different (Fig. 3), and the concentration of Cu is much lower than that of Zn. As the beneficial elements (Cu and Zn) must be in a suitable concentration range, exceeding concentration will cause damage to the organism itself (Prabhu et al., 2016).

For U, its mobility is enhanced in the high state (uranyl carbonate), and it is often affected by the presence of carbonates (Charette and Sholkovitz, 2006; Gonneea et al., 2014). The high state U forms a stable uranyl carbonate with the carbonate, which facilitates its existence in solution.

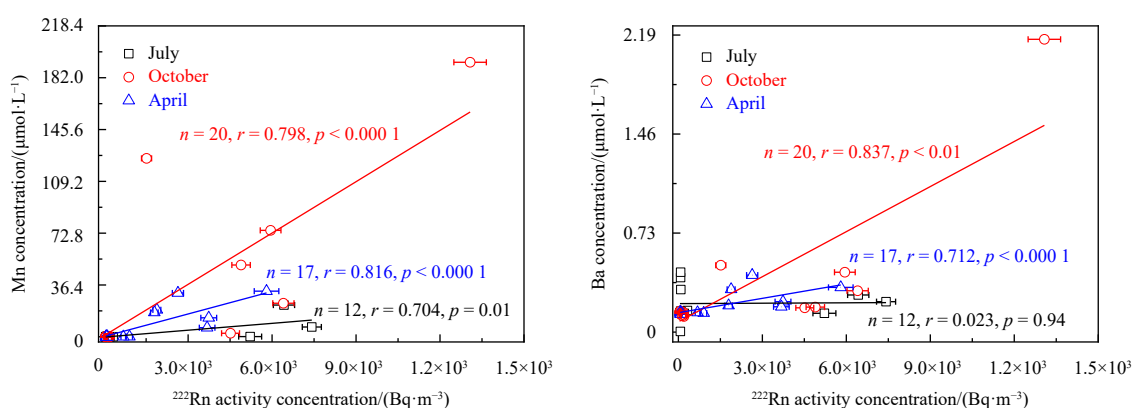


**Fig. 9.**  $^{222}\text{Rn}$  activity versus Mn and Ba concentrations in intertidal groundwater and seawater.

### 4.3 Significant seasonal variations on SGD-driven metal fluxes

The three supply metals in which we were interested contribute to the local environment's metal budget. They may have an impact on the surrounding ecosystem and therefore cannot be ignored. However, our findings demonstrate that using the results of a single sampling to predict annual metal fluxes will result in a significant mistake because the SGD derived metal fluxes fluctuate periodically. For example, the maximum Fe flux was 0.288 mmol/(m<sup>2</sup>·d) (October) and the minimum was 0.079 mmol/(m<sup>2</sup>·d) (April). If the result of a single measurement was used, the October result would be 3.6 times higher than that of April. The difference between Mn in the season with the highest flux and the season with the lowest flux may be estimated using a similar method to be 5.5 times, whereas the difference between Ba flux will be 15 times.

Zn, U and Cr show source-sink reversal, which will directly lead to the estimation error for the long-term metal fluxes estimation driven by SGD. So we prefer to use multi-quarter averages value to (average flux over three quarters) instead of single-quarter calculations, which prevented over or under-estimates of the metal fluxes gap by SGD especially for the supply metals and removal metal. This average method can be effective representation of annual SGD-driven metal flux, although the method is relatively simple, it is effective. Using this method, we get that metal fluxes contributed by SGD are comparable to either riverine or atmospheric source (metal sediment diffusion flux is included in the SGD). Figure 6 shows that the flux of Mn of groundwater is much larger than that of rivers in any season, and the fluxes of Fe and Ba of groundwater are comparable to or larger than those from rivers. The dry deposition fluxes of Fe and Mn in the adjacent sea area (South Yellow Sea, adjacent to this sea area) were 0.11 mmol/(m<sup>2</sup>·d) and 0.003 mmol/(m<sup>2</sup>·d), respectively (Yuan et al., 2012). The deposition fluxes of Fe and Mn were either smaller or comparable to the SGD contribution. It should be noted that the atmospheric deposition rate mentioned above was the total deposition rate, if only the soluble deposition part is much smaller (the magnitude is nmol/(m<sup>2</sup>·d)) (Hsu et al., 2010). The largest atmospheric deposition fluxes were used for comparison. Comparison of the results with the metal fluxes contributed by other end-member shows that SGD is a significant source of Mn, Fe and Ba. These metals have an important impact on the growth and survival of nearshore organisms (e.g., Fe). For example, Fe plays an important role in enzymatic reactions, photosynthesis, or other synthetic reactions, and primary productivity can also be affected by Fe limitations (Zhang et al., 2019).

Cu may be a limiting factor for aquaculture in this area due to the Cu sink (the capture of benthic organisms' results in the continued removal of Cu) in the STE. Therefore, it is necessary to further study and evaluate the trace element content of the cultured organisms here to determine whether the area is Cu deficient.

### 5 Conclusions

Strong seasonal variations of SGD-derived metal fluxes have been discovered, and they are divided into three categories (supply metals, remove metal and dynamically balance metals). Fe, Mn and Ba are supply metals and their seasonal variation may be related to the variation of DOC concentration and the proportion of fresh groundwater. Cu is remove metal and this may be related to aquaculture. Pb, Zn, U and Cr are dynamic balance metals, which show complex seasonal changes. In a word, ignoring the impact of seasonal changes on the metal fluxes driven by SGD will significantly affect the correct estimation of the metal contribution of SGD and the understanding of the nearshore metal cycle.

### References

- Alorda-Kleinglass A, Garcia-Orellana J, Rodellas V, et al. 2019. Remobilization of dissolved metals from a coastal mine tailing deposit driven by groundwater discharge and porewater exchange. *Science of the Total Environment*, 688: 1359–1372, doi: [10.1016/j.scitotenv.2019.06.224](https://doi.org/10.1016/j.scitotenv.2019.06.224)
- Amato E D, Simpson S L, Remaili T M, et al. 2016. Assessing the effects of bioturbation on metal bioavailability in contaminated sediments by diffusive gradients in thin films (DGT). *Environmental Science & Technology*, 50(6): 3055–3064, doi: [10.1021/acs.est.5b04995](https://doi.org/10.1021/acs.est.5b04995)
- Beck A J, Cochran J K, Sañudo-Wilhelmy S A. 2009. Temporal trends of dissolved trace metals in Jamaica Bay, NY: importance of wastewater input and submarine groundwater discharge in an urban estuary. *Estuaries and Coasts*, 32(3): 535–550, doi: [10.1007/s12237-009-9140-5](https://doi.org/10.1007/s12237-009-9140-5)
- Berelson W, McManus J, Coale K, et al. 2003. A time series of benthic flux measurements from Monterey Bay, CA. *Continental Shelf Research*, 23(5): 457–481, doi: [10.1016/s0278-4343\(03\)00009-8](https://doi.org/10.1016/s0278-4343(03)00009-8)
- Burnett W C, Bokuniewicz H, Huettel M, et al. 2003. Groundwater and pore water inputs to the coastal zone. *Biogeochemistry*, 66(1): 3–33, doi: [10.1023/B:Biog.0000006066.21240.53](https://doi.org/10.1023/B:Biog.0000006066.21240.53)
- Burnett W C, Dulaiova H. 2003. Estimating the dynamics of groundwater input into the coastal zone via continuous radon-222 measurements. *Journal of Environmental Radioactivity*, 69(1–2): 21–35, doi: [10.1016/s0265-931x\(03\)00084-5](https://doi.org/10.1016/s0265-931x(03)00084-5)
- Charette M A, Sholkovitz E R. 2006. Trace element cycling in a subterranean estuary: part 2. Geochemistry of the pore water. *Geochimica et Cosmochimica Acta*, 70(4): 811–826, doi: [10.1016/j.gca.2005.10.019](https://doi.org/10.1016/j.gca.2005.10.019)
- Charette M A, Sholkovitz E R, Hansel C M. 2005. Trace element cycling in a subterranean estuary: part 1. Geochemistry of the permeable sediments. *Geochimica et Cosmochimica Acta*, 69(8): 2095–2109, doi: [10.1016/j.gca.2004.10.024](https://doi.org/10.1016/j.gca.2004.10.024)
- Chen Xiaogang, Zhang Fenfen, Lao Yanling, et al. 2018. Submarine groundwater discharge-derived carbon fluxes in mangroves: an important component of blue carbon budgets?. *Journal of Geophysical Research: Oceans*, 123(9): 6962–6979, doi: [10.1029/2018jc014448](https://doi.org/10.1029/2018jc014448)
- de Souza Machado A A, Spencer K, Kloas W, et al. 2016. Metal fate and effects in estuaries: a review and conceptual model for better understanding of toxicity. *Science of the Total Environment*, 541: 268–281, doi: [10.1016/j.scitotenv.2015.09.045](https://doi.org/10.1016/j.scitotenv.2015.09.045)
- Degenhardt J, Merder J, Heyerhoff B, et al. 2021. Cross-shore and depth zonations in bacterial diversity are linked to age and source of dissolved organic matter across the intertidal area of a sandy beach. *Microorganisms*, 9(8): 1720, doi: [10.3390/microorganisms9081720](https://doi.org/10.3390/microorganisms9081720)
- Du Laing G, Meers E, Dewispelaere M, et al. 2009. Effect of water table level on metal mobility at different depths in wetland soils of the scheldt estuary (belgium). *Water, Air, and Soil Pollution*, 202(1): 353–367, doi: [10.1007/s11270-009-9982-2](https://doi.org/10.1007/s11270-009-9982-2)
- Gonnee M E, Charette M A, Liu Qian, et al. 2014. Trace element geochemistry of groundwater in a Karst subterranean estuary (Yucatan Peninsula, Mexico). *Geochimica et Cosmochimica Acta*, 132: 31–49, doi: [10.1016/j.gca.2014.01.037](https://doi.org/10.1016/j.gca.2014.01.037)
- Hagedorn B, Tsuda M. 2022. Radon and salinity mass balance constraints on groundwater recharge on a semi-arid island (Catalina, California). *Water*, 14(7): 1068, doi: [10.3390/w14071068](https://doi.org/10.3390/w14071068)
- Hao Youyou. 2021. Distribution characteristics and influencing factors of biogenic elements in the Aojiang Estuary and adjacent waters under the background of tidal flat shellfish aquaculture (in Chinese)[dissertation]. Shanghai: East China Normal University
- Hong Qingquan, Cai Pinghe, Geibert W, et al. 2018. Benthic fluxes of metals into the Pearl River Estuary based on <sup>224</sup>Ra/<sup>228</sup>Th disequilibrium: from alkaline earth (Ba) to redox sensitive elements (U, Mn, Fe). *Geochimica et Cosmochimica Acta*, 237:

- 223–239, doi: [10.1016/j.gca.2018.06.036](https://doi.org/10.1016/j.gca.2018.06.036)
- Hsu S C, Wong G T F, Gong G C, et al. 2010. Sources, solubility, and dry deposition of aerosol trace elements over the East China Sea. *Marine Chemistry*, 120(1–4): 116–127, doi: [10.1016/j.marchem.2008.10.003](https://doi.org/10.1016/j.marchem.2008.10.003)
- Kim I, Kim G. 2011. Large fluxes of rare earth elements through submarine groundwater discharge (SGD) from a volcanic island, Jeju, Korea. *Marine Chemistry*, 127(1–4): 12–19, doi: [10.1016/j.marchem.2011.07.006](https://doi.org/10.1016/j.marchem.2011.07.006)
- Kim I, Kim G. 2015. Role of colloids in the discharge of trace elements and rare earth elements from coastal groundwater to the ocean. *Marine Chemistry*, 176: 126–132, doi: [10.1016/j.marchem.2015.08.009](https://doi.org/10.1016/j.marchem.2015.08.009)
- Li Maomao, Kong Fanlong, Li Yue, et al. 2020. Ecological indication based on source, content, and structure characteristics of dissolved organic matter in surface sediment from Dagu River Estuary, China. *Environmental Science and Pollution Research*, 27(36): 45499–45512, doi: [10.1007/s11356-020-10456-1](https://doi.org/10.1007/s11356-020-10456-1)
- Luijendijk E, Gleeson T, Moosdorf N. 2020. Fresh groundwater discharge insignificant for the world's oceans but important for coastal ecosystems. *Nature Communications*, 11(1): 1260, doi: [10.1038/s41467-020-15064-8](https://doi.org/10.1038/s41467-020-15064-8)
- Mayfield K K, Eisenhauer A, Santiago Ramos D P, et al. 2021. Groundwater discharge impacts marine isotope budgets of Li, Mg, Ca, Sr, and Ba. *Nature Communications*, 12(1): 148, doi: [10.1038/s41467-020-20248-3](https://doi.org/10.1038/s41467-020-20248-3)
- Mendiguchía C, Moreno C, Manuel-Vez M P, et al. 2006. Preliminary investigation on the enrichment of heavy metals in marine sediments originated from intensive aquaculture effluents. *Aquaculture*, 254(1–4): 317–325, doi: [10.1016/j.aquaculture.2005.10.049](https://doi.org/10.1016/j.aquaculture.2005.10.049)
- Moosdorf N, Böttcher M E, Adyasari D, et al. 2021. A state-of-the-art perspective on the characterization of subterranean estuaries at the regional scale. *Frontiers in Earth Science*, 9: 601293, doi: [10.3389/feart.2021.601293](https://doi.org/10.3389/feart.2021.601293)
- Nakajima T, Sugimoto R, Tominaga O, et al. 2018. Fresh and recirculated submarine groundwater discharge evaluated by geochemical tracers and a seepage meter at two sites in the Seto Inland Sea, Japan. *Hydrology*, 5(4): 61, doi: [10.3390/hydrology5040061](https://doi.org/10.3390/hydrology5040061)
- Nimptsch J, Woelfl S, Osorio S, et al. 2015. Tracing dissolved organic matter (DOM) from land-based aquaculture systems in North Patagonian streams. *Science of the Total Environment*, 537: 129–138, doi: [10.1016/j.scitotenv.2015.07.160](https://doi.org/10.1016/j.scitotenv.2015.07.160)
- O'Connor A E, Canuel E A, Beck A J. 2022. Drivers and seasonal variability of redox-sensitive metal chemistry in a shallow subterranean estuary. *Frontiers in Environmental Science*, 9: 613191, doi: [10.3389/fenvs.2021.613191](https://doi.org/10.3389/fenvs.2021.613191)
- O'Connor A E, Krask J L, Canuel E A, et al. 2018. Seasonality of major redox constituents in a shallow subterranean estuary. *Geochimica et Cosmochimica Acta*, 224: 344–361, doi: [10.1016/j.gca.2017.10.013](https://doi.org/10.1016/j.gca.2017.10.013)
- O'Connor A E, Luek J L, McIntosh H, et al. 2015. Geochemistry of redox-sensitive trace elements in a shallow subterranean estuary. *Marine Chemistry*, 172: 70–81, doi: [10.1016/j.marchem.2015.03.001](https://doi.org/10.1016/j.marchem.2015.03.001)
- Peng Tong, Zhu Zhuoyi, Du Jinzhou, et al. 2021. Effects of nutrient-rich submarine groundwater discharge on marine aquaculture: a case in Lianjiang, East China Sea. *Science of the Total Environment*, 786: 147388, doi: [10.1016/j.scitotenv.2021.147388](https://doi.org/10.1016/j.scitotenv.2021.147388)
- Prabhu A J, Schrama J W, Kaushik S J. 2016. Mineral requirements of fish: a systematic review. *Reviews in Aquaculture*, 8(2): 172–219, doi: [10.1111/raq.12090](https://doi.org/10.1111/raq.12090)
- Ruiz-González C, Rodellas V, Garcia-Orellana J. 2021. The microbial dimension of submarine groundwater discharge: current challenges and future directions. *FEMS Microbiology Reviews*, 45(5): fuab010, doi: [10.1093/femsre/fuab010](https://doi.org/10.1093/femsre/fuab010)
- Santana-Casiano J M, González-Dávila M, González A G, et al. 2014. Characterization of phenolic exudates from *Phaeodactylum tri-cornutum* and their effects on the chemistry of Fe(II)–Fe(III). *Marine Chemistry*, 158: 10–16, doi: [10.1016/j.marchem.2013.11.001](https://doi.org/10.1016/j.marchem.2013.11.001)
- Santos I R, Burnett W C, Chanton J, et al. 2009. Land or ocean?: assessing the driving forces of submarine groundwater discharge at a coastal site in the Gulf of Mexico. *Journal of Geophysical Research: Oceans*, 114(C4): C04012, doi: [10.1029/2008jc005038](https://doi.org/10.1029/2008jc005038)
- Santos I R, Burnett W C, Misra S, et al. 2011a. Uranium and barium cycling in a salt wedge subterranean estuary: the influence of tidal pumping. *Chemical Geology*, 287(1–2): 114–123, doi: [10.1016/j.chemgeo.2011.06.005](https://doi.org/10.1016/j.chemgeo.2011.06.005)
- Santos I R, Chen Xiaogang, Lecher A L, et al. 2021. Submarine groundwater discharge impacts on coastal nutrient biogeochemistry. *Nature Reviews Earth & Environment*, 2(5): 307–323, doi: [10.1038/s43017-021-00152-0](https://doi.org/10.1038/s43017-021-00152-0)
- Santos I R, Lechuga-Deveze C, Peterson R N, et al. 2011b. Tracing submarine hydrothermal inputs into a coastal bay in Baja California using radon. *Chemical Geology*, 282(1–2): 1–10, doi: [10.1016/j.chemgeo.2010.12.024](https://doi.org/10.1016/j.chemgeo.2010.12.024)
- Santos I R, Peterson R N, Eyre B D, et al. 2010. Significant lateral inputs of fresh groundwater into a stratified tropical estuary: evidence from radon and radium isotopes. *Marine Chemistry*, 121(1–4): 37–48, doi: [10.1016/j.marchem.2010.03.003](https://doi.org/10.1016/j.marchem.2010.03.003)
- Shahid M, Pinelli E, Dumat C. 2012. Review of Pb availability and toxicity to plants in relation with metal speciation; role of synthetic and natural organic ligands. *Journal of Hazardous Materials*, 219–220: 1–12, doi: [10.1016/j.jhazmat.2012.01.060](https://doi.org/10.1016/j.jhazmat.2012.01.060)
- Shi Xiangming, Wei Lin, Hong Qingquan, et al. 2019. Large benthic fluxes of dissolved iron in China coastal seas revealed by <sup>224</sup>Ra/<sup>228</sup>Th disequilibria. *Geochimica et Cosmochimica Acta*, 260: 49–61, doi: [10.1016/j.gca.2019.06.026](https://doi.org/10.1016/j.gca.2019.06.026)
- Shine J P, Ika R, Ford T E. 1998. Relationship between oxygen consumption and sediment-water fluxes of heavy metals in coastal marine sediments. *Environmental Toxicology and Chemistry*, 17(11): 2325–2337, doi: [10.1002/etc.5620171125](https://doi.org/10.1002/etc.5620171125)
- Smaal A C, Vonck A P M A. 1997. Seasonal variation in C, N and P budgets and tissue composition of the mussel *Mytilus edulis*. *Marine Ecology Progress Series*, 153: 167–179, doi: [10.3354/meps153167](https://doi.org/10.3354/meps153167)
- Taniguchi M, Ishitobi T, Shimada J. 2006. Dynamics of submarine groundwater discharge and freshwater-seawater interface. *Journal of Geophysical Research: Oceans*, 111(C1): C01008, doi: [10.1029/2005jc002924](https://doi.org/10.1029/2005jc002924)
- Trezzi G, Garcia-Orellana J, Rodellas V, et al. 2016. Submarine groundwater discharge: a significant source of dissolved trace metals to the North Western Mediterranean Sea. *Marine Chemistry*, 186: 90–100, doi: [10.1016/j.marchem.2016.08.004](https://doi.org/10.1016/j.marchem.2016.08.004)
- Wang Xiaoxiong, Chen Xiaogang, Liu Jianan, et al. 2021. Radon traced seasonal variations of water mixing and accompanying nutrient and carbon transport in the Yellow-Bohai Sea. *Science of the Total Environment*, 784: 147161, doi: [10.1016/j.scitotenv.2021.147161](https://doi.org/10.1016/j.scitotenv.2021.147161)
- Wang Qianqian, Li Hailong, Zhang Yan, et al. 2019. Evaluations of submarine groundwater discharge and associated heavy metal fluxes in Bohai Bay, China. *Science of the Total Environment*, 695: 133873, doi: [10.1016/j.scitotenv.2019.133873](https://doi.org/10.1016/j.scitotenv.2019.133873)
- Wang Xiaona, Wu Ying, Jiang Zengjie, et al. 2017. Quantifying aquaculture-derived dissolved organic matter in the mesocosms of Sanggou Bay using excitation-emission matrix spectra and parallel factor analysis. *Journal of the World Aquaculture Society*, 48(6): 909–926, doi: [10.1111/jwas.12409](https://doi.org/10.1111/jwas.12409)
- Waska H, Brumsack H J, Massmann G, et al. 2019. Inorganic and organic iron and copper species of the subterranean estuary: origins and fate. *Geochimica et Cosmochimica Acta*, 259: 211–232, doi: [10.1016/j.gca.2019.06.004](https://doi.org/10.1016/j.gca.2019.06.004)
- Yuan Huamao, Song Jinming, Li Xuegang, et al. 2012. Distribution and contamination of heavy metals in surface sediments of the South Yellow Sea. *Marine Pollution Bulletin*, 64(10): 2151–2159, doi: [10.1016/j.marpolbul.2012.07.040](https://doi.org/10.1016/j.marpolbul.2012.07.040)

- Zhang Jing, Kattner G, Koch B P. 2019. Interactions of trace elements and organic ligands in seawater and implications for quantifying biogeochemical dynamics: a review. *Earth-Science Reviews*, 192: 631–649, doi: [10.1016/j.earscirev.2019.03.007](https://doi.org/10.1016/j.earscirev.2019.03.007)
- Zhang Yan, Li Hailong, Wang Xuejing, et al. 2016. Estimation of submarine groundwater discharge and associated nutrient fluxes in eastern Laizhou Bay, China using  $^{222}\text{Rn}$ . *Journal of Hydrology*, 533: 103–113, doi: [10.1016/j.jhydrol.2015.11.027](https://doi.org/10.1016/j.jhydrol.2015.11.027)
- Zhang Yan, Wang Xuejing, Xue Yan, et al. 2022. Advances in the study of submarine groundwater discharge (SGD) in China. *Science China: Earth Sciences*, 65(10): 1948–1960, doi: [10.1007/s11430-021-9946-x](https://doi.org/10.1007/s11430-021-9946-x)

---

## Supplementary information:

**Fig. S1.** The time series variations of DO, pH, temperature, salinity, DSI, DIC and DOC during three seasons (July, October, April).

**Fig. S2.** Temporal variation of groundwater flux and  $F_{\text{net}}$ .

**Table S1.** Parameters used in the  $^{222}\text{Rn}$ -Box model.

**Table S2.** Summary of parameters of different water masses bodies in different seasons.

**Table S3.** The specific data of metal fluxes.

The supplementary information is available online at <https://doi.org/10.1007/s13131-023-2232-4> and <http://www.aosocean.com/>. The supplementary information is published as submitted, without typesetting or editing. The responsibility for scientific accuracy and content remains entirely with the authors.